DA1

Whole heart histological reconstruction: promises and challenges

F. Mahmood, A. Garny, R. Burton, F. Mason and P. Kohl

Department of Physiology, Anatomy and Genetics, University of Oxford, Oxford, UK

Introduction

Histo-anatomy is a major determinant of heart function, affecting behaviours such as spread of excitation, stress/strain distribution, contraction/relaxation, and coronary perfusion, to name but a few. A detailed quantitative understanding of cardiac structure-function interrelation in norm and disease therefore requires an equally detailed insight into the histo-anatomical make-up of the whole organ (Burton et al. 2006). Thus far, partial histological reconstructions have been used in conjunction with diffusion tensor magnetic resonance (MR) imaging, to provide local high-resolution information for MR validation. However, these data sets are inherently limited by the resolution of the MR techniques used, usually yielding voxel dimensions for the whole heart in the range of 10^{-3}-10^{-4} m. Here, we demonstrate an approach to mapping cardiac anatomy at 10^{-5}-10^{-6} m resolution for an entire rabbit heart.

Preparation

A female New Zealand white rabbit was terminally anesthetised using 140 mg/kg intravenous sodium pentobarbital, in accordance with the Home Office Animals (Scientific Procedures) Act of 1986. The heart was excised, rinsed in heparinised (25 IU/L) Tyrode solution, and cardioplegically arrested using high potassium (20 mM KCl) modified Tyrode. The heart was fixed using freshly prepared Karnovsky's fixative (a 2% paraformaldehyde / 2.5% glutaraldehyde mix). After high-resolution anatomical MR imaging, the heart was dehydrated using increasing concentrations of alcohol and wax embedded over a three-week period. Longitudinal sections of the entire heart were taken at 10 μm thickness using a heavy duty sledge type microtome (Leica SM2400). Sections were relaxed in a water bath (Leica HI 12110) at 40°C before being placed onto numbered 3-aminopropyltriethoxysilan coated slides. Each section was stained using the Masson's Trichrome technique, before being mounted using DPX and left to dry in a fume hood overnight.

Imaging

All sections were imaged using a Leica QWin workstation and Leica QGO software to obtain mosaic images of the entire section (the largest sections were up to ~40 mm long and ~20 mm wide). Using a 10x objective, final in-plane pixel resolution was 1.1 μm x 1.1 μm. A total of 1,850 sections were produced (whole heart thickness was 18.5 mm), yielding voxel dimensions of 10^{-5} x 10^{-6} x 10^{-6} m. Imaging time depended on tissue section size and varied from 30 s to over 10 min. Individual images were stored as bitmaps (BMP) ranging from a few hundred megabytes (MB) to just under 2 gigabytes (GB) in size.

Challenges

While developing the above method, a number of challenges were identified, including:

- Difficulty in avoiding air bubbles in the complex cardiac structure during embedding (mild vacuum and changes in sample orientation needed).
- Incomplete tissue relaxation (15-20 min per section can be required).
- Terabytes (TB) of disk space are necessary to store the images. Compression and conversion to the PNG format of individual images was explored; the time required (1-3 min for compressing and 20-50 s for decompressing 1-2 GB images, respectively) made this unattractive for local use, though it may be necessary to facilitate sharing of information over the Internet (the compression results in an image file size reduction to 50-70% of the original).
- Larger images cannot be rendered natively in Microsoft Windows. To this end, we developed a BMP viewer which can be downloaded from http://mef.physiol.ox.ac.uk/Software/BMPViewer.exe. The software creates a thumbnail that is automatically generated when selecting a BMP file. A second window is used to render only part of the image at its native resolution. Clicking anywhere on the thumbnail updates the contents of the native viewer, which can also be panned around the image.

The total volume of histological information for one heart was just over 1.3 TB. This is currently being used, in conjunction with the MR data obtained prior to sectioning, for reconstruction of partial tissue areas, such as ventricular tissue wedges or papillary muscle (Plotkowiak et al., 2008). In the process, techniques for whole heart reconstruction are generated.

Burton RABR et al. Three-dimensional models of individual cardiac histo-anatomy: tools and challenges, Annals of the New York Academy of Sciences 2006/1080:301-319.

Plotkowiak M et al. High performance computer simulations of cardiac electrical function based on high resolution MRI datasets. Lecture Notes for Computer Science 2008 (in press).

Supported by the BBSRC and the BHF.

Where applicable, the authors confirm that the experiments described here conform with The Physiological Society ethical requirements.

DA2

Ca^{2+}-sensitive microelectrodes are well sensitive to barium ions inside snail (Helix aspersa) neurones

R.C. Thomas

PDN, University of Cambridge, Cambridge, UK

Barium has long been used to study calcium influx, since it passes through calcium channels more readily than calcium itself (Eckert & Lux, 1976). It also inhibits potassium channels, making it easier to isolate the inward current. Barium entry into non-excitable cells has been studied using Fura-2 over the last decade (e.g. Bakowski & Parekh, 2007) yet little seems to be known about intracellular Ba^{2+} ions in nerve cells. I will show that Ca^{2+}-sensitive microelectrodes (CaSM) made with the sensor ETH 129 (Ammann et al, 1987) appear to be almost equally sensitive to Ba^{2+} as to Ca^{2+}, as shown in the illustrative result in Fig 1. This experiment was done on a snail neurone in an isolated ganglion preparation using techniques as described in Thomas (2002) and Thomas & Postma (2007). Strangely, CaSMs

made with this sensor were originally described as very much less sensitive to Ba^{2+} than to Ca^{2+} ions.
In the experiment illustrated a large neurone was penetrated first with a CaSM, then with two conventional CsCl-filled microelectrodes to measure the membrane potential and clamp it at -50 mV, and finally with a pH-sensitive microelectrode (pHSM). Every few minutes the cell was depolarised to zero for 5 s. This opened calcium and potassium channels. Initially the cell was bathed in normal 7 mM Ca snail Ringer and depolarised several times, only the last of which is shown. Then the superfusate was changed to a Ringer in which all the calcium was replaced by barium. The CaSM potential changed little, but the depolarisation-induced elevations in CaSM potential were larger than seen in calcium, and were accompanied by a larger change in pH_i. The recovery of the CaSM signal after each presumed barium influx was slower that after each calcium influx. The clamp current during the depolarisations was outward in calcium, but inward in barium. The effects of barium Ringer were reversed on return to normal calcium Ringer.

The CaSMs were made from quartz micropipettes silanized at about 450°C for 10 min, while the pH-sensitive microelectrodes were made from borosilicate glass micropipettes silanized at about 250°C. The quartz micropipettes were backfilled with 1 mM $CaCl_2$, and then frontfilled by suction with a 0.1-0.3 mm column of cocktail (Thomas 2002) and left for at least an hour before use. The pHSMs are made similarly with the cocktail Fluka 95297.
Thomas RC (2002) *J gen.Physiol* **120**, 567-579.

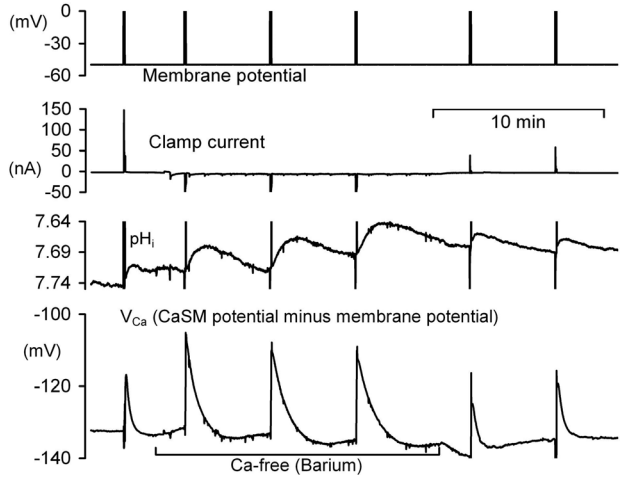

Fig 1. Recording of part of an experiment on a snail neurone in an isolated suboesophageal ganglion. The recording shows, from the top, membrane potential, clamp current, (pH_i) and the potential of the intracellular CaSM referred to the membrane potential, (V_{Ca}). V_{Ca} values of -120 mV and -140 mV correspond to [Ca^{2+}] of about 300 and 60 nM respectively. Where indicated, the ganglion was superfused with snail Ringer in which the normal 7 mM $CaCl_2$ was replaced with 7 mM $BaCl_2$.

Ammann D et al (1987)*Pflugers Arch* **409**,223-228.

Bakowski D & Parekh AB (2007)*Cell Calcium* **42**, 333-339.

Eckert R & Lux HD (1976) *J Physiol* **254**, 129-151.

Thomas RC & Postma M (2007) *Cell Calcium* **41**, 365-378.

I am very grateful to the Wellcome Trust.

Where applicable, the authors confirm that the experiments described here conform with The Physiological Society ethical requirements.

DA3

A simple gas-powered microforge for fire-polishing suction pipettes

C.J. Schwiening and L. Caldwell

Department of Physiology, Development and Neuroscience, University of Cambridge, Cambridge, UK

Most microforges suitable for fire-polishing micropipettes are based on resistive electrical heating elements. Such elements, especially those found on homemade microforges, have a number of problems when used for heating large amounts of glass e.g. when polishing suction electrodes (diameter ~15 μm). First, the resistive element is large making the use of high-power objectives difficult. Second, the element moves as it heats up requiring readjustment of its position. Third, large amounts of waste heat (radiant and conductive) are produced; this can damage objectives. Fourth, when run at high outputs they have a limited lifespan. Fifth, elements based on platinum are expensive.
Here we demonstrate a very simple and cheap gas-powered microforge with a high (4 W) output of usable heat. It is based upon a disposable cigarette lighter, a length of plastic tubing and a micropipette (GC100T Harvard Apparatus) with a large (~600 μm) tip. To assemble the microforge, the metal cover over the gas nozzle was removed and the lighter gas flow set near to its minimum value (4-10 mg min^{-1}, equivalent to 70-170 μmoles min^{-1} of butane or ~2 ml min^{-1}). A plastic tube (internal diameter ~0.9 mm) was connected to the gas nozzle and at its other end a 1 mm diameter glass micropipette with a broken tip was inserted. A small wedge can be used to lock the gas flow open. Once the gas is ignited the micropipette tip melts and the gas flow maintains the patent lumen.
The gas emitted from the micropipette is easy to light and burns with a clear blue diffusion flame when adjusted to ~2 ml min^{-1}. The flame is reasonably stable (it will withstand air currents of ~0.5 m s^{-1} Beaufort 0), but some care needs to be taken to shield it from draughts. It can be positioned in any orientation, although we use it mounted horizontally on an inverted microscope allowing the waste heat to escape upwards. A standard disposable cigarette lighter should provide between 3-8 h use.
We are using this microforge to fire polish suction pipettes from an internal diameter of ~300 μm down to 15 μm (Figure 1). The main advantage of this gas-powered microforge is that a much larger proportion of the total heat output is available for fire-polishing. Whilst nichrome, Kanthal and platinum melt at ~1400°C, ~1300°C and ~1770°C respectively a butane flame can burn continuously at ~1300°C. The radiant energy from the flame is relatively low compared with a glowing electrical element, allowing it to be positioned directly above the objective and the flame does not move. The majority of the heating occurs as the suction pipette tip approaches within ~10 μm of the flame allowing a reasonably good control of the fire-polishing process without needing to switch off the flame.

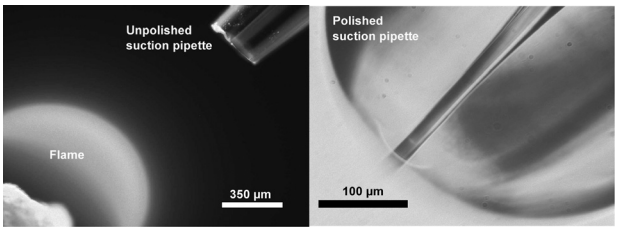

Figure 1. Photomicrographs of the gas flame and suction pipette. The left image was taken at low magnification and shows the static gas flame and the cut, unpolished pipette. The right image, at higher magnification, shows the suction pipette polished to an internal diameter of 15 μm.

Where applicable, the authors confirm that the experiments described here conform with The Physiological Society ethical requirements.

DA4

A demonstration of image analysis software based on kanban principles for exploring large data sets

C. Schwiening

Department of Physiology, Development and Neuroscience, University of Cambridge, Cambridge, UK

Using both conventional imaging and confocal systems it is possible to collect large data sets rapidly. For a number of reasons the exploration and analysis of these data sets can be far more time consuming than the original experiments. First, the large quantity of data takes a significant amount of time to load into memory. Second, the stepwise iteration of regions of interest (ROI) through the data set can be computationally expensive. Third, with many commercial software packages the analysis involves making intermediate files of identical size (for example when using a spatial filter) that further expand the data set and cannot be easily modified once made.

Here I present a compiled Visual Basic (Microsoft) program that overcomes some of these problems. The program allows for ROI analysis of large data sets. It implements a simple set of ideas to produce significant speed and flexibility gains when compared with most commercial software.

The software uses some principles of the kanban business model (Sugimori et al., 1977) more commonly known as 'just-in-time' (JIT). The main benefit of this model is that large amounts of unnecessary 'stock' are not held. Instead only that which is instantaneously required is obtained. In computing terms this means that when a file is opened only the first image is displayed – this can be done almost instantly. Then, when a ROI is drawn only the data from that region is read from the file. Furthermore, if the data are to be plotted, only the frames that can be plotted on the screen are analysed.

For example, an image series lasting 10 min acquired at 512x512 pixel resolution at 25 frames s^{-1} using an 8-bit model will generate at least 3.9 GB of data (15,000 frames). Typically, such images might cover an area of 100 μm x 100 μm (pixel size ~0.2 μm). A circular region of interest of, for instance a cell body might be 10 μm in diameter and would therefore comprise ~2000 pixels. This represents ~0.8% of the total number of pixels in the frame. An initial overview of the mean intensity for that region, on a standard 1024x768 monitor, requires data to be calculated from every 1/15th frame (1000 data points). Thus, the data actually required is only 2 MB in total. This is ~0.05% (1/2000th) of the complete data set. If the analysis process is rate limited by the data transfer rate – which is frequently the case – this kanban process could yield a 2000-times faster analysis. Of course, the analysis of smaller regions in longer time-series would produce greater gains whereas for larger regions in shorter time-series smaller gains would be expected.

Optimization of the kanban process, by the underlying memory cache of the operating system, means that once data are extracted for a given region subsequent modifications to the analysis occur without large amounts of data transfer. Thus, the kanban-driven acquisition occurs with the same short latency as if the whole data set had been loaded into memory. Furthermore, operations on the data such as spatial and temporal filtering are applied as necessary to the data 'on the fly' – this is again a kanban principle. This means that the filtering can easily be adjusted and data replotted without the need for the production of intervening files.

Part of the JIT process is that certain operations are predicted, and those not associated with a time overhead are performed in advance. For example, numerical ROI data are available on the clipboard immediately after plotting so that they can be exported to other analysis software.

The software also implements the simple idea of non-contiguous pixel-based ROIs. This allows pixels from anywhere in the image to be selected and combined into a single functional region.

Currently, data files from Leica (LIF), Zeiss (LSM), TIF, BMP and JPG files can be analysed. The program allows background subtraction, single and dual wavelength ratios, sub-pixel resolution image shifting (based upon a linear-interpolation algorithim), temporal and spatial smoothing, basic curve fitting and calibration of ionic data. The program will function with large (>2 GB data sets) on a wide range of Windows machines even with very modest (256 MB) memory specifications taking data across Ethernet networks.

Sugimori Y *et al.*(1977) *Int J Prod Res*, **15**, 553-564.

Where applicable, the authors confirm that the experiments described here conform with The Physiological Society ethical requirements.

DA5

Simultaneous ratiometric fluorescence measurement of regional intracellular calcium and pH in rat cerebellar Purkinje neurones

O. Larina and C.J. Schwiening

Department of Physiology, Development and Neuroscience, University of Cambridge, Cambridge, UK

There is a close linkage between intracellular pH changes and transmembrane calcium fluxes in many cell types. To understand these associations better it is often desirable to measure pH and [Ca^{2+}] simultaneously at a sub-cellular level. Here we report that a mixture of HPTS and Fura-red loaded into a

neurone can allow such measurements to be made on a confocal microscope.

Intracellular pH was calculated from the ratio of HPTS fluorescence (500-580 nm) when excited with alternating 405 nm and 488 nm light. Fura-red has a much larger Stoke's shift and fluoresces at >600 nm, and when excited with alternating 405 nm and 488nm light produces a ratio indicating [Ca^{2+}].

We find that a mixture of 125 μM HPTS and 62.5 μM Fura-red, when loaded into whole-cell patch-clamped neurones, allows both calcium and pH to be monitored simultaneously in subcellular regions with no discernable cross-talk between the two dyes (see Figure 1).

The usefulness of this technique may depend upon the type of confocal, and the available filters. Our Leica SP5, with its electronically tuneable beam splitter and spectral emission, allows the two dyes to be separated. However, experiments on our Zeiss LSM510, using just 488 nm excitation, show some overlap between the two dyes.

The calcium- and pH-sensitive images are acquired synchronously, using identical wavelengths for the excitation; this allows us to rule out some artefacts when comparing calcium and pH.

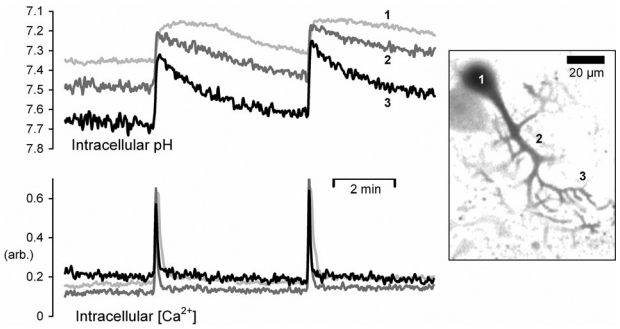

Figure 1. Simultaneous ratiometric recordings of intracellular pH and intracellular [Ca^{2+}] from a whole-cell patch-clamped Purkinje neurone in a cerebellar slice in HEPES buffered Ringer. The cell was depolarized twice to 0 mV for 1s from a holding potential of –60 mV. Data are shown for three regions; the cell body, primary dendrite and secondary dendrites. The patch solution was based on CsCl and contained 125 μM HPTS and 62.5 μM Fura-red.

We thank the MRC for providing equipment and financial support.

Where applicable, the authors confirm that the experiments described here conform with The Physiological Society ethical requirements.

PL1

Hormones as epigenetic signals in developmental programming

A.L. Fowden

Department of Physiology, Development and Neuroscience, University of cambridge, Cambridge, UK

Many recent human epidemiological observations and studies in experimental animals have shown that, in mammals, adult phenotype can be altered by environmental conditions experienced during prenatal and early postnatal development (1). Environmental factors, such as nutrition, temperature, light exposure and housing conditions, all alter intrauterine development with phenotypic consequences for a wide range of physiological systems later in life (2). The process by which environmental conditions during early life permanently alter tissue structure and function is known as developmental programming (3). However, the nature of the epigenetic signals controlling the phenotypic outcome of environmental challenges early in development remains unclear. In invertebrates and lower order vertebrates like insects, anurans, reptiles and birds, hormones have a central role in triggering key developmental events and often mediate the effects of environmental factors on metamorphosis and cell differentiation. Hormones also regulate development in mammalian fetuses (4). Specific hormones, such as insulin, insulin like growth factors (IGFs), glucocorticoids and thyroid hormones, have been shown to control growth of the mammalian fetus overall and its individual tissues by actions on cell proliferation and differentiation. These hormones also act as signals of nutrient plenty (eg insulin, IGFs, thyroid hormones) or nutrient insufficiency (eg catecholamines, glucocorticoids) and, thereby, communicate environmental conditions to the developing feto-placental tissues (4).

Environmentally-induced endocrine signals to the fetus arise in three main ways. First, they may be due to transplacental transfer of maternal hormones released in response to the environmental challenge per se. Second, they may reflect changes in placental hormone synthesis and/or metabolism, which alter the bioavailability of hormones in both the fetal and maternal circulations. Finally, they may occur by direct activation of the fetal endocrine glands, particularly late in gestation when the endocrine axes are relatively mature and responsive to stimuli. The environmentally induced-changes in endocrine signalling alter fetal development both directly and indirectly. Indirect actions involve changes in the distribution and metabolic fate of nutrients and in the growth and nutrient transfer capacity of the placenta. Direct actions include changes in gene expression for enzymes, growth factors, transporters, ion channels, intracellular signalling molecules and hormone receptors, which, in turn, may affect the response to subsequent environmental challenges. At the molecular level, hormones may affect DNA methylation, promotor usage, transcription, RNA stability, translation and/or post-translational processing of the protein products (5). The specific phenotypic consequences of altered hormone exposure in utero depend on the type, severity and duration of the endocrine change which, in turn, is determined by the specific environmental challenge and stage of development. Hormones can, therefore, act as epigenetic signals in developmental programming and may provide a final common pathway by which different environmental factors can have similar phenotypic outcomes. In addition, by altering the phenotype of specific tissues like the placenta, hormones provide a mechanism of transmitting the memory of early events to the fetus later in gestation, which may determine tissue development long after the original environmental

Barker DJP (2001). Br. Med. Bull. 60 69-88.

McMillen IC & Robinson JS (2005) Physiol. Rev. 85 571-633.

Lucas A (1991). Ciba Foundation Symposium 156 38-50.

Fowden AL & Forhead AJ (2004). Reproduction 127 515-526.

Waterland RA & Michels KB (2007) Ann. Rev. Nutr. 27 363-388.

6. Fowden AL et al. (2008) J. Neuroendocrinol. 20 439-450

Authors have confirmed where relevant, that experiments on animals and man were conducted in accordance with national and/or local ethical requirements.

PL3

What causes heart attacks and strokes: seeing is believing

P.L. Weissberg

British Heart Foundation, London, UK

Together, heart attacks and strokes cause more deaths in the UK than any other disease. Both are caused by a disease called atherosclerosis that involves the build up of fatty deposits, called plaques, on the inside of the blood vessels that supply the heart and brain with essential oxygen. Blood clots can suddenly

develop on plaques causing the blood flow to cease completely. If this happens in the heart, a part of the heart dies – a heart attack. A similar phenomenon in the blood vessels feeding the brain causes a stroke. As a result of recent research we now understand the cellular processes that lead to the development of atherosclerotic plaques and, more importantly, what causes them to suddenly form a blood clot. This has led to the development of new treatments aimed at preventing heart attacks and strokes. However, because most people beyond middle age have some degree of atherosclerosis without knowing it – often there are no symptoms until a blood clot forms - we urgently need a clinical test to identify dangerous plaques and treat them before they cause a heart attack or a stroke. In this lecture I will describe the cellular processes that lead to dangerous plaques and how new, state of the art imaging techniques are being used to identify them before they cause a major problem.

Authors have confirmed where relevant, that experiments on animals and man were conducted in accordance with national and/or local ethical requirements.

PL4

The role of calcium in the regulation and mis-regulation of cardiac excitation contraction-coupling

A.W. Trafford

Unit of Cardiac Physiology, University of Manchester, Manchester, UK

The dependence of cardiac muscle on extracellular calcium for the generation of force has been known since the experiments of Ringer in 1883. However, in recent decades, the application of electrophysiological and epifluorescence methods to studies on isolated cardiac myocytes has also led to an appreciation of the critical role that intracellular calcium plays in regulating cardiac force development. The arrival of the action potential causes a small amount of calcium to enter the cell primarily via L-type calcium channels. This then triggers the release of a much larger amount of calcium from the specialised intracellular calcium store, the sarcoplasmic reticulum (SR), thus giving rise to the systolic calcium transient and ultimately activation of the myofilaments and contraction. Relaxation is brought about by the combination of calcium reuptake in to the SR and calcium efflux from the cell primarily via the electrogenic sodium calcium exchanger.

Using quantitative techniques the dependence of the systolic calcium transient on SR calcium has been determined to be approximately cubic; thus small changes in SR calcium content will have profound effects on the systolic calcium transient and ultimately the generation of force by the heart. Furthermore, should the amount of calcium stored within the SR exceed a threshold level then spontaneous (non-triggered) release of calcium occurs and this is an established mechanism by which ventricular arrhythmias are initiated. It is therefore vital that the SR calcium content is carefully controlled. Fortunately, the heart has evolved an inherently simple feedback system through which this is achieved whereby the systolic calcium transient controls both calcium entry and efflux across the cell surface membrane and thus ultimately SR calcium content.

Several physiological manoeuvres, for example β-adrenergic stimulation, alter cardiac contractility by changing the amplitude of the systolic calcium transient through modulation of this feedback system to effect increases of SR calcium content. Additionally, in the case of heart failure, alterations to the mechanisms controlling SR calcium content lead to a reduction in the amount of calcium stored in the SR and therefore a decrease in contractility.

Thus, understanding the vital role that calcium plays in regulating cardiac excitation contraction and how this is perturbed in various disease settings holds the promise of providing novel means by which we may be able to, on the one hand, increase SR calcium content to improve contractility for example in heart failure whilst on the other hand, preventing unwanted potentially arrhythmogenic aberrant release of calcium from the sarcoplasmic reticulum.

Supported by grants from The British Heart Foundation, Wellcome Trust and BBSRC

Authors have confirmed where relevant, that experiments on animals and man were conducted in accordance with national and/or local ethical requirements.

PL5

***In vitro* fertilization**

R.G. Edwards

Reproductive BioMedicine Online, Cambridge, UK and University of Cambridge, Cambridge, UK

Human IVF, which began with the successful birth of the first test tube baby in 1978, was the culmination of several decades of medical and scientific research. Having conducted research into many aspects of mammalian reproductive biology, by the mid-1960s in my laboratory at Cambridge University we studied human oocytes obtained from pathology specimens, and successfully matured and developed these *in vitro*. In 1968 I met Patrick Steptoe, who was able to retrieve fresh human oocytes via a laparoscope, and with the help of our colleague Jean Purdy, we started to study these oocytes. We were soon able to fertilize human eggs and culture embryos for up to 9 days, observing beautiful hatched blastocysts *in vitro*. However, it took 10 years of dedicated and persistent effort, in the face of disappointment, failure, and considerable controversy and criticism from our peers, before we were rewarded with the birth of Louise Brown in 1978. A new medico-scientific discipline has evolved and developed from these beginnings. The application of IVF techniques and technology has resulted in the birth of several million babies so far, and now even gives hope to cancer patients with the possibility of preserving their fertility. It has also opened the door to significant discoveries in genetics, cell and molecular biology. Offshoots of IVF technology, from preimplantation genetic diagnosis to stem cell therapy and tissue regeneration, now hold promise for significantly improving in the quality of human life and the alleviation of degenerative diseases in the future.

In the field of scientific research, application of assisted reproductive techniques in animal systems has helped to unravel the

fundamental steps involved in fertilization, gene programming and expression, regulation of the cell cycle and patterns of differentiation.

The first babies born after transfer of embryos that had been frozen and thawed were born in 1984-85, and cryopreservation of embryos as well as semen became routine. Experiments with cell cultures and co-culture allowed the development of stage-specific media optimized for embryo culture to the blastocyst stage. Advances in techniques and micromanipulation technology led to the establishment of assisted fertilization (intracytoplasmic sperm injection) by a Belgian team led by André Van Steirteghem and including Gianpiero Palermo (Palermo et al. 1992) by the mid 1990s. Other microsurgical interventions were then introduced, such as assisted hatching and embryo biopsy for genetic diagnosis. Gonadal tissue cryopreservation, *in vitro* oocyte maturation and embryonic stem cell culture are now under development as therapeutic instruments and remedies for the future.

Applications in Veterinary Science

The first live calves resulting from bovine IVF were born in the USA in 1981. This further milestone in reproductive biotechnology inspired the development of IVF as the next potential commercial application of assisted reproduction in domestic species, following on from artificial insemination and conventional transfer of embryos produced *in vivo* from superovulated donors. The assisted reproductive techniques continued to be refined so that by the 1990s IVF was integrated into routine domestic species breeding programmes. Equine IVF has also been introduced into the world of horse breeding (although reproductive technology procedures cannot be used for thoroughbreds). China used artificial insemination to produce the first giant panda cub in captivity in 1963, and assisted reproduction is now used in the rescue and propagation of endangered species, from pandas and large cats to dolphins. Artificial insemination, and, in some cases, IVF are used routinely in specialist zoos throughout the world.

Somatic cell nuclear transfer into enucleated oocytes has created 'cloned' animals in several species, the most famous being Dolly the sheep, who was born in Edinburgh in 1997 and was euthanized at an early age in February 2003, after developing arthritis and progressive lung disease.

Advances in molecular biology and biotechnology continue to be applied in assisted reproductive technology. Preimplantation genetic diagnosis, introduced in 1988, is used to screen embryos for sex-linked diseases or autosomal mutations in order to exclude chromosomally abnormal embryos from transfer. Molecular biology techniques can identify chromosomes with the use of fluorescently labelled probes for hybridization, or amplify DNA from a single blastomere using the polymerase chain reaction. This technique is also used for gender selection, now used routinely in animal breeding programmes.

Authors have confirmed where relevant, that experiments on animals and man were conducted in accordance with national and/or local ethical requirements.

C1

Transient and sustained synaptic activity in the retina of zebrafish imaged using a genetically encoded calcium indicator

E. Dreosti, B. Odermatt and L. Lagnado

Neurobiology, MRC Laboratory of Molecular Biology, Cambridge, UK

Retinal bipolar cells play a key role in the processing of the visual signal because they are the only neurons transmitting information directly from photoreceptors providing the input to ganglion cells, which deliver the output. The ON class of bipolar cells are depolarized by an increase in light intensity, while OFF cells are hyperpolarized. Bipolar cells also contribute to the temporal filtering of the visual input into sustained and transient channels responding preferentially to slow or fast changes in light intensity (Masland, 2001). It is still unclear how the ribbon-type synapses of bipolar cells transmit voltage signals of opposite polarities and different kinetics.

To monitor synaptic activity of bipolar cells, operating within the intact retinal circuit, we have made transgenic zebrafish expressing a new genetically-encoded reporter of synaptic activity. This reporter, SyGCaMP2, is composed of the calcium-sensitive fluorescent construct GCaMP2 (Tallini, 2006) fused to the synaptic vesicle protein synaptophysin. SyGCaMP2 was put under control of a promoter driving expression in ribbon synapses and calcium signals monitored across tens to hundreds of terminals in the inner retina by multiphoton microscopy. Zebrafish 9-12 days post-fertilization were anaesthetised by immersion in 0.016% MS222, immobilized in low melting agarose and injected with α-bungarotoxin (2mg/ml). Both spontaneous and light-driven activity were monitored through all the strata of the inner plexiform layer at rates up to 200 Hz and across one stratum at 1 kHz.

We observed two basic types of presynaptic calcium signal in response to light: slow, sustained changes and faster calcium "spikes". Sustained increases or decreases in calcium were observed in ON or OFF cells respectively, and were maintained throughout exposure to a step of light. These slow calcium signals are expected to modulate the rate at which vesicles are cycled through rounds of exocytosis and endocytosis (Lagnado et al., 1996). Calcium "spikes" were observed in both ON and OFF cells, rising to a peak in about 50 ms and declining in seconds. These fast signals are likely to reflect regenerative electrical activity through L-type calcium channels in the synaptic terminal (Burrone and Lagnado, 1997), which will trigger fast, transient, modes of exocytosis (Burrone, 2000). Individual bipolar cells transmitting in different strata of the IPL did not necessarily generate presynaptic calcium signals with the same kinetics: sustained signals were observed in some terminals and transient signals in others. These observations suggest that the basic unit for the generation of transient signals from the bipolar cells is the synaptic terminal rather than the whole neuron.

Masland RH (2001). Nat Neurosci 4, 877-886.

Tallini YN et al. (2006). Proc Natl Acad Sci USA 103, 4753-4758.

Lagnado L et al. (1996). Neuron 17, 957-967.

Burrone J & Lagnado L (1997). J Physiol 15, 571-584.

Burrone J et al. (2000) J Neurosci 20, 568-578.